PHYSICAL REVIEW E **107**, 064126 (2023)

Entropy-driven phases at high coverage adsorption of straight rigid rods on three-dimensional cubic lattices

P. M. Pasinetti,[1] A. J. Ramirez-Pastor,[1,*] and E. E. Vogel[2,3]

[1]*Departamento de Física, Instituto de Física Aplicada (INFAP), Universidad Nacional de San Luis - CONICET, Ejército de Los Andes 950, D5700HHW San Luis, Argentina*
[2]*Departamento de Física, Universidad de La Frontera, Casilla 54-D, Temuco 481180, Chile*
[3]*Center for the Development of Nanoscience and Nanotechnology (CEDENNA), 9170124 Santiago, Chile*

(Received 7 March 2023; accepted 7 June 2023; published 22 June 2023)

Combining Monte Carlo simulations and thermodynamic integration method, we study the configurational entropy per site of straight rigid rods of length k (k-mers) adsorbed on three-dimensional (3D) simple cubic lattices. The process is monitored by following the dependence of the lattice coverage θ on the chemical potential μ (adsorption isotherm). Then, we perform the integration of $\mu(\theta)$ over θ to calculate the configurational entropy per site of the adsorbed phase $s(k,\theta)$ as a function of the coverage. Based on the behavior of the function $s(k,\theta)$, different phase diagrams are obtained according to the k values: $k \leqslant 4$, disordered phase; $k = 5, 6$, disordered and layered-disordered phases; and $k \geqslant 7$, disordered, nematic and layered-disordered phases. In the limit of $\theta \rightarrow 1$ (full coverage), the configurational entropy per site is determined for values of k ranging between 2 and 8. For $k \geqslant 6$, MC data coincide (within the statistical uncertainty) with recent analytical predictions [D. Dhar and R. Rajesh, Phys. Rev. E **103**, 042130 (2021)] for very large rods. This finding represents the first numerical validation of the expression obtained by Dhar and Rajesh for d-dimensional lattices with $d > 2$. In addition, for $k \geqslant 5$, the values of $s(k, \theta \rightarrow 1)$ for simple cubic lattices are coincident with those values reported in [P. M. Pasinetti *et al.*, Phys. Rev. E **104**, 054136 (2021)] for two-dimensional (2D) square lattices. This is consistent with the picture that at high densities and $k \geqslant 5$, the layered-disordered phase is formed on the lattice. Under these conditions, the system breaks to 2D layers, and the adsorbed phase becomes essentially 2D. The 2D behavior of the fully covered lattice reinforces the conjecture that the large-k behavior of entropy per site is superuniversal, and holds on d-dimensional hypercubical lattices for all $d \geqslant 2$.

DOI: 10.1103/PhysRevE.107.064126

I. INTRODUCTION

Systems of hard rods and cylinders interacting with only excluded volume interactions between them have long been of interest to the statistical mechanics community [1]. In the case of lattice models, the study of linear hard rods (or straight rigid k-mers) started with the work of Flory [2] and Zwanzig [3]. The k-mers are modeled as rigid objects containing k identical units, with each one occupying a lattice site. The distance between k-mer units is assumed to be equal to the lattice constant; hence exactly k sites are occupied by a k-mer when adsorbed. The only interaction between different rods is hard-core exclusion (no site can be occupied by more than one k-mer) and the rods can orient only along one of the d directions of a d-dimensional hypercubic lattice.

With increasing density, and for large enough k-mer sizes, the system of rigid rods undergoes transitions from a low-density orientationally disordered phase to an intermediate-density nematically ordered phase to a high-density disordered phase where the nematic order disappears [4]. The first transition, usually referred to as isotropic-nematic phase transition, belongs to the Ising or more generally Potts universality class, depending on the number of different possible directions of nematic order: Ising universality class for square lattices [5] and three-state Potts universality class for triangular [5] and honeycomb [6] lattices. The existence of the transition has been rigorously proved in two dimensions (2D) [7], and has been seen in the exactly soluble case of k-mers on treelike lattices [8]. The first transition has also been detected by machine learning [9] and information theory [10,11].

The relaxation time increases very quickly as the density increases. Usual Monte Carlo (MC) simulations use local deposition-evaporation moves. In this scheme, the states at high densities are sampled inefficiently due to the presence of highly jammed long-lived metastable configurations. As a result of these limitations, most of the unknown is in regard to the high-density disordered (HDD) phase, which has been less studied than the low and intermediate phases. Recent results suggested the transition from the nematic to the HDD phase to be discontinuous [12]. The study in Ref. [12] continues a previous paper by Dhar and Rajesh [13], where the configurational entropy of the HDD phase has been investigated for a $L \times M$ square lattice fully covered by straight rigid rods of length k. By combining the lower [13] and upper [14] bounds obtained for entropy, Dhar and Rajesh showed that, in the limit of large k, the configurational entropy per site tends to $Ak^{-2} \ln k$, with $A = 1$. In addition, based on a perturbative series expansion, the authors conjectured that the large-k

---

[*] Author to whom correspondence should be addressed: antorami@unsl.edu.ar

©2023 American Physical Society

behavior of entropy per site is superuniversal, and continues to hold on d-dimensional hypercubical lattices for all $d \geqslant 2$.

In a recent work from our group [15], MC simulations in the grand canonical ensemble, supplemented by thermodynamic integration, were used to first calculate the configurational entropy of the adsorbed phase as a function of the coverage, and then to explore the different phases (and orientational transitions) that appear on the surface with increasing the density of adsorbed k-mers. In the limit of $\theta \rightarrow 1$ (full coverage), the configurational entropy was obtained for values of k ranging between 2 and 10. The study showed that Dhar and Rajesh's theoretical results [13] and simulation data coincide, within the statistical uncertainty, in the range $k \geqslant 6$. The numerical results in Ref. [15] validate the dependence of the configurational entropy on k obtained in Ref. [13] and allow for an accurate determination of its applicability range. The theoretical predictions in Ref. [13] have also been corroborated by transfer-matrix analysis [16].

In this work, we extend the study of Ref. [15] to three-dimensional (3D) lattices. For this purpose, extensive MC simulations supplemented by thermodynamic integration method have been used to calculate the configurational entropy per site of the adsorbed phase $s(k, \theta)$ as a function of coverage ($0 \leqslant \theta \leqslant 1$). The process has been carried out for straight rigid k-mers ($2 \leqslant k \leqslant 8$) adsorbed on 3D simple cubic lattices. The behavior of the configurational entropy per site at full coverage as a function of the k-mer size was obtained and compared with the recently reported expression $s(k, \theta = 1)/k_B = k^{-2} \ln k$ ($k \rightarrow \infty$) [13]. The MC study presented here represents, to our best knowledge, the first numerical validation of the theoretical predictions of Rajesh and Dhar [13] in dimensions greater than 2. Previous studies in Refs. [15,16] were restricted to 2D lattices.

On the other hand, by comparing the configurational entropy $s(k, \theta)$ with the ones corresponding to square lattices and fully aligned systems [whose calculation reduces to the one-dimensional (1D) case], the different phase transitions that occur on the surface were identified: (i) $k \leqslant 4$, the system is disordered at all densities; (ii) for $k = 5$ and 6, there is no nematic phase, and a single transition occurs from a disordered 3D phase to a layered-disordered phase. In the layered-disordered phase, the system breaks up into very weakly interacting 2D planes within which the rods are disordered; and (iii) for $k \geqslant 7$, the adsorbed phase shows nematic order at intermediate density. In addition, the system breaks to 2D layers at high density. The obtained results are discussed and compared with previous data in the literature for monodispersed hard rods of length k adsorbed on 3D simple cubic lattices [17,18].

Our study, based on the behavior of the configurational entropy of the adsorbed phase, allows to clearly visualize the 2D character of the layered-disordered phase appearing for large k-mers and coverage close to 1. This 2D behavior of the fully covered lattice reinforces the conjecture that the large-k behavior of entropy per site is superuniversal, and holds on d-dimensional hypercubical lattices for all $d \geqslant 2$ [13].

This paper is organized as follows. The calculation methodology is presented in Sec. II. Most relevant results are presented in the form of plots which are immediately discussed in Sec. III. Conclusions are summarized in Sec. IV.

II. METHODOLOGY. FUNCTIONS AND VARIABLES

A. Simulations: Adsorption-desorption algorithm

Lattice gas simulations of rods of length k (linear k-mers) were done in the grand canonical ensemble using a efficient algorithm presented by Kundu *et al.* [19,20], which was designed to overcome the slow sampling at high coverage and was generalized in this work to cubic lattices. The temperature T, chemical potential μ, and system size L are kept fixed, whereas the number of particles N is allowed to fluctuate through nonlocal changes, i.e., insertion and/or removal of several k-mers at the time (in contrast to the standard Metropolis algorithm).

Given a particular configuration of k-mers on the cubic lattice, distributed in the three possible directions (d_1, d_2, d_3), a Monte Carlo step (MCs) begins with the choice of one direction, for example d_1, followed by the removal of all the k-mers in that direction. In this way, we have L^2 rows (or rings considering the periodic boundary conditions) along the d_1 direction, consisting in intervals of different length formed by contiguous empty sites. Such intervals are separated from each other by sites occupied by k-mers along the other two directions.

Each interval on these rows could be filled independently by new k-mers in the d_1 direction, provided that the interval length be greater or equal to k. Given one of these intervals of length l ($\geqslant k$), it is very simple to calculate the equilibrium probability (given the temperature and chemical potential) of having the first k sites of the interval occupied by a k-mer [21]. Such probability could be previously calculated and stored, for intervals of different lengths (from 0 to L) to increase the computational performance. From these probabilities it is possible to fill all the intervals in the d_1 direction of the system with new equilibrium configurations of k-mers and empty sites. The MCs is completed by repeating the same procedure of emptying and refilling along the other two directions, d_2 and d_3.

Besides the just described removal and filling processes of k-mers along the three directions, it is found that the sampling and equilibrating times can be considerably reduced by adding a patch or tile rotation step. In this process, a site (x, y, z) and a direction d_i are randomly selected. If that site is the corner of a set of k parallel and contiguous k-mers forming a tile of $k \times k$ sites on a plane normal to the d_i direction, then the tile is rotated 90 degree of that direction (in this rotation only the $k \times k$ sites above mentioned are affected). Otherwise, the attempt is rejected.

Then, the complete MCs will comprise removing and filling processes along each of the three possible directions, followed by the patch rotation process which will be repeated L^3 times, i.e., one per site in average. A detailed discussion of the original algorithm can be found in Refs. [19,20]. The algorithm thus defined proved to be ergodic and to satisfy the detailed balance principle.

A cubic lattice of $M = L^3$ sites with periodic boundary conditions was used. The relation L/k was fixed to 60. The equilibrium is reached typically after $r_0 = 10^6$ MCs. Then, simple averages are computed over other $r = 10^6$ configurations. In our MC simulations, we varied the chemical potential and monitored the density θ,

$$\theta = \frac{k\langle N\rangle}{M}, \tag{1}$$

where the bracket $\langle \dots \rangle$ denotes the average over the r MC simulation runs after equilibrium is settled.

B. Configurational entropy of the adsorbed phase: Thermodynamic integration method

As mentioned in Sec. I, the configurational entropy of the adsorbed phase S was calculated by using the thermodynamic integration method [15,22–28]. In the grand canonical ensemble, the method relies upon integration of the chemical potential μ on coverage along a reversible path between an arbitrary reference state and the desired state of the system. This calculation also requires the knowledge of the total energy U for each coverage. Thus, for a system made of N particles on M lattice sites, we have

$$\mu = \left(\frac{\partial F}{\partial N}\right)_{M,T}, \tag{2}$$

where $F = U - TS$ is the Helmholtz free energy and S is the configurational entropy. It follows that,

$$\begin{aligned} S(k, M, N, T) = {} & S_0(k, M, N_0, T) \\ & + \frac{U(k, M, N, T) - U(k, M, N_0, T)}{T} \\ & - \frac{1}{T}\int_{N_0}^{N} \mu dN. \end{aligned} \tag{3}$$

In the present case, $U(k, M, N, T) = 0$ and the determination of the entropy in the reference state, $S_0(k, M, N_0, T)$, is trivial [$S_0(k, M, N_0, T) = 0$ for $N_0 = 0$]. Then, after writing the last equation in terms of intensive variables, the configurational entropy per site ($s = S/M$) results in

$$\frac{s(k, \theta, T)}{k_B} = -\frac{1}{k_B T}\int_0^{\theta} \frac{\mu}{k}\, d\theta, \tag{4}$$

where $\theta = kN/M$ and k_B is the Boltzmann constant. Given that all chemical potentials are being measured in units of k_BT, all results will be independent of the temperature. Accordingly, for the rest of the paper we will use $s(k, \theta)$ to denote the configurational entropy per site (for simplicity we will drop the "T" label).

The curve of μ versus θ can be got by following the adsorption-desorption algorithm described in Sec. II A [see Eq. (1)]. The integration required in Eq. (4) is carried out using the well-known trapezoidal rule [29]. Two error sources affect the entropy calculations: (i) the simulation error associated with the measurement of the adsorption isotherm; and (ii) the error inherent to the integration method. Regarding the simulation error, each point in the adsorption isotherm curve is obtained with an error of the order of 10^{-5}. Moreover, the error coming from the integration method can be controlled by choosing appropriately the number of integration points n_μ (number of discrete values in the adsorption isotherm) [29]. In the present study, the curve $\mu(\theta)$ contains $n_\mu = 61$ points. With these values of the parameters, the simulation error is of the order of 10^{-3} and the integration error is negligible compared to the simulation error. This results in the total error for the entropy per site at full coverage that will be reported in the next section (see the sixth column in Table I).

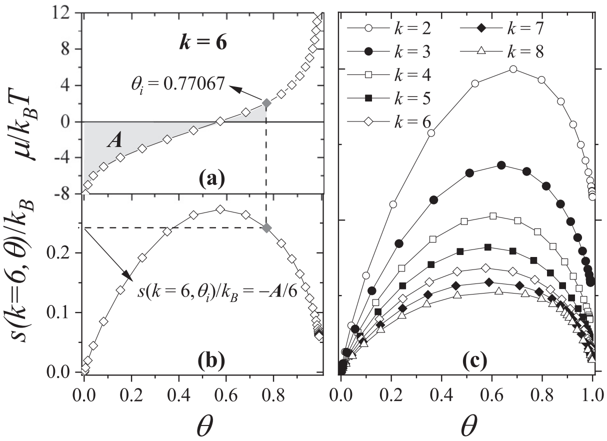

FIG. 1. Chemical potential (a) and configurational entropy per site (b) as function of coverage for $k = 6$. Parts (a) and (b) illustrate the implementation of the thermodynamic integration method. The value of A is -1.4512. The adsorption isotherm in (a) was measured in the range from $\mu/k_BT = -15$ to $\mu/k_BT = 20$. A shorter range is shown ($\mu/k_BT = -8$ to $\mu/k_BT = 12$) for a better visualization. (c) Configurational entropy per site as function of coverage for different values of k: $k = 2$, open circles; $k = 3$, solid circles; $k = 4$, open squares; $k = 5$, solid squares; $k = 6$, open diamonds; $k = 7$, solid diamonds; and $k = 8$, open triangles.

III. RESULTS AND DISCUSSION

We begin by getting the configurational entropy per site as a function of coverage $s(k, \theta)/k_B$ through Eq. (4). The calculation is carried out in two stages. In the first stage, the coverage dependence of $\mu(\theta)/k_BT$ is evaluated following the MC procedure described in the previous section. A typical curve of μ/k_BT versus θ, obtained for $k = 6$ is depicted in Fig. 1(a). A smooth coverage dependence is observed as a result of the large number of averaged configurations. The error bars are smaller than the size of the symbols, which tells of the accuracy of the simulated data.

In the second stage, the curves of $\mu(\theta)/k_BT$ are numerically integrated. To apply the thermodynamic integration method, a point θ_i is chosen on the curve of $\mu(\theta)/k_BT$, and the integral $A = \int_0^{\theta_i} (\mu/k_BT)\, d\theta$ is calculated. Let us consider, as an example, the adsorption isotherm for $k = 6$ [Fig. 1(a)] and $\theta_i = 0.77067$ (gray diamond). In this case, $A = -1.4512$ and the corresponding entropy per site yields $s(k = 6, \theta_i)/k_B = -A/6 = 0.24187$ [see the gray diamond in Fig. 1(b)]. By repeating the procedure for all values of θ_i, the curve of entropy versus coverage can be calculated.

The methodology described in Figs. 1(a) and 1(b) was repeated for $2 \leqslant k \leqslant 8$, the results are shown in Fig. 1(c).

TABLE I. Configurational entropy per site for straight rigid k-mers at full coverage. First column, k-mer size ($2 \leqslant k \leqslant 8$); second column, theoretical predictions from Eq. (8) (the values are rounded to five decimal places) [13]; third column, MC results obtained in Ref. [15] for 2D square lattices; and fourth column, MC results obtained in the present work for 3D simple cubic lattices. Statistical errors are in the last digit and are indicated in parentheses.

	Entropy per site at full coverage, $s(k, \theta = 1)/k_B$		
k	Eq. (8) [13]	MC, square lattices [15]	MC, simple cubic lattices (this work)
2	0.17329	0.293(2)	0.451(2)
3	0.12207	0.159(2)	0.203(3)
4	0.08664	0.101(2)	0.111(3)
5	0.06438	0.070(3)	0.071(3)
6	0.04977	0.052(3)	0.050(3)
7	0.03971	0.040(3)	0.040(4)
8	0.03249	0.032(3)	0.031(4)

As mentioned in Sec. II B, the configurational entropy curves were calculated for $n_\mu = 61$ points. Only 31 points are shown in the figure for clarity. The general features of the coverage dependence of the entropy per site are the following. Approaching the limit $\theta = 0$ the entropy tends to zero. For very low densities, $s(k, \theta)/k_B$ is an increasing function of θ; it reaches a maximum at θ_m, then decreases monotonically to a finite value for $\theta = 1$.

As shown in previous work [15], the behavior of entropy as a function of coverage appears as a useful property to explore the possible ordered phases present in systems with purely steric interactions for increasing values of the density. In the case of straight rigid k-mers adsorbed on 3D cubic lattices (with three allowed orientations), Vigneshwar *et al.* [17] and Gschwind *et al.* [18] reported the existence of different surface phases with increasing coverage: isotropic phase (IP), nematic phase (NP) and layered-disordered phase (LDP). In the isotropic phase, the system is disordered and the k-mers are equally distributed in the three directions of space. The nematic state is characterized by a big domain of parallel k-mers oriented along one of the lattice directions. The k-mers of the other two orientations have smaller, roughly equal concentrations. In the layered-disordered phase, the density of rods of one orientation is strongly suppressed, breaking the system into weakly coupled layers. In each one of these layers, the rods form local domains (or islands) of parallel k-mers without long-range orientational order.

The system does not present long-range order (the system is disordered) at all densities for $k \leqslant 4$ [17]. This can be visualized for $k = 3$ in Fig. 2(a), where the configurational entropy per site calculated by the thermodynamic integration method (line and spheres) is presented. For comparison, the figure also includes the curves of (i) the configurational entropy per site calculated from fundamental measure theory (FMT) [18] (red solid line); (ii) the configurational entropy per site obtained analytically for a fully aligned system of 3-mers (dashed line); and (iii) the configurational entropy per site got by the thermodynamic integration method for straight rigid 3-mers adsorbed on 2D square lattices with two allowed orientations (line and squares).

In 1944, Guggenheim proposed an interesting method to calculate the combinatory term in the canonical partition function [30]. Later, in a valuable contribution, DiMarzio developed an approximate method of counting the number of ways, Ω, to pack together linear polymer molecules of arbitrary shape and of arbitrary orientations [31]. In the case of allowing only those orientations for which the molecules fit exactly onto the lattice and for an isotropic distribution, the value of Ω reduces to the value obtained previously by Guggenheim [30]. In this limit, the configurational entropy

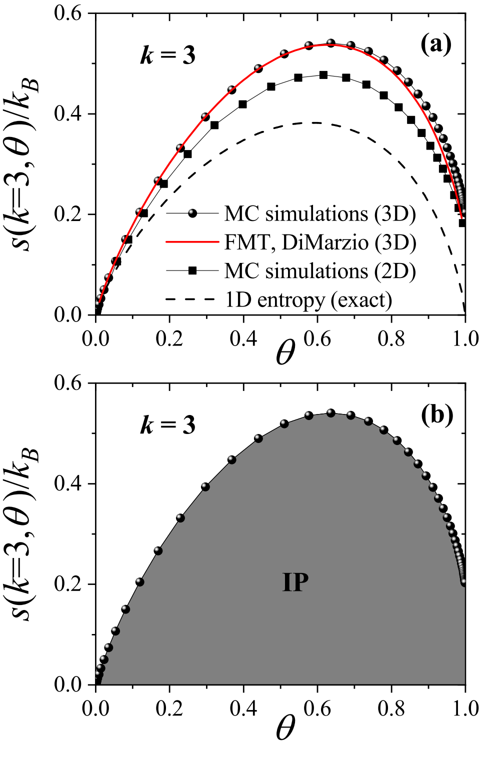

FIG. 2. (a) Configurational entropy per site as function of coverage for straight rigid 3-mers ($k = 3$) adsorbed on three different geometries: 3D simple cubic lattices (line and spheres); 2D square lattices (line and squares) and 1D chains (solid line). Line and symbols correspond to results obtained by MC simulations (complemented by the thermodynamic integration method), the dashed line represents analytical results according to expression in Eq. (6) with $k = 3$, and the red solid line indicates results from FMT [DiMarzio's theory, Eq. (5) with $k = 3$]. The system is characterized by an isotropic phase (IP) over the entire range of values of k [part (b)].

per site for a system of straight rigid k-mers adsorbed on a lattice of connectivity γ can be written as

$$\frac{s(k,\theta,\gamma)}{k_B} = \left[\frac{\gamma}{2} - \frac{(k-1)}{k}\theta\right] \ln \left[\frac{\gamma}{2} - \frac{(k-1)}{k}\theta\right] - \frac{\theta}{k} \ln \frac{\theta}{k} - (1-\theta)\ln(1-\theta) + \left(\theta - \frac{\gamma}{2}\right) \ln \frac{\gamma}{2}. \tag{5}$$

The equivalence of the DiMarzio entropy to exact solutions on Bethe-like lattices was investigated in Refs. [8,32]. An alternative theoretical route for treating hard particles on lattices was proposed by Lafuente and Cuesta [33,34]. The authors extended the Rosenfeld's FMT [35,36] to lattice models by constructing a density functional for d-dimensional mixtures of parallel hard hypercubes on a simple hypercubic lattice. For the case of rod models in 2D and 3D, the FMT functional and its bulk properties were worked out in Ref. [37]. It turns out that lattice FMT is equivalent to DiMarzio's treatment [31] or rods on Bethe-like lattices with coordination numbers 4 and 6 (representing 2D and 3D, respectively) [8].

In the fully aligned state, the k-mers (trimers in the case of Fig. 2) align along one of the three directions and the entropy of this nematic state having density θ can be reduced to the entropy of a one-dimensional problem [21]:

$$\frac{s_{1D}(k,\theta)}{k_B} = \left[1 - \frac{(k-1)}{k}\theta\right] \ln \left[1 - \frac{(k-1)}{k}\theta\right] - \frac{\theta}{k} \ln \frac{\theta}{k} - (1-\theta)\ln(1-\theta). \tag{6}$$

In addition, the system breaks in 2D layers in the layered phase and the entropy of this state reduces to the entropy of straight rigid k-mers adsorbed on 2D square lattices. As observed in Fig. 2(a), FMT presents an excellent agreement with the simulation results, showing that FMT is a good approximation for a state with zero nematic order. MC and FMT curves are indistinguishable up to $\theta < 0.7$. Above $\theta \approx 0.7$, small differences between MC and FMT predictions are observed. In addition, the 3D entropy is greater than those of 2D and 1D systems over the entire range of coverage. It is important to notice that at no point the curves in this figure cross or overlap. This finding shows that with $k = 3$, and following the principle of maximum entropy, the adsorbed phase reaches neither nematic nor layered order at any point when the density varies between 0 and 1. Accordingly, the system is characterized by an isotropic phase over the entire range of values of θ [part (b)].

The behavior of these systems changes when reaching $k = 5$ and 6 [17]. In these cases, the adsorbed phase presents disorder at low and intermediate densities, and goes to a high density layered-disordered phase. Next, this picture will be analyzed in terms of entropy.

In Fig. 3(a), the configurational entropy per site has been studied for 3D, 2D, and 1D systems with $k = 6$. As in the previous figure, the solid line corresponds to the direct evaluation of Eq. (6) with $k = 6$. Line and symbol curves represent MC simulation data: 3D simple cubic lattices (line and spheres); and 2D square lattices (line and squares). The inset shows a zoom of the main figure in the range $0.8 \leqslant \theta \leqslant 1$.

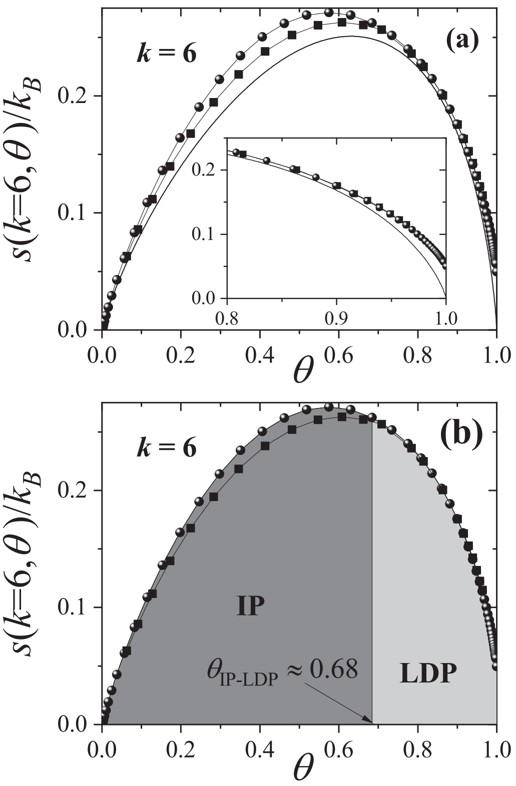

FIG. 3. (a) Same as Fig. 2(a) but for $k = 6$. The inset displays the departure of the theoretical expression [Eq. (6), solid line] from 2D and 3D simulations (line and symbols) at high coverage. IP and LDP regions are shown in part (b).

The 3D system does not show nematic order for all values of density and, consequently, the 3D entropy is higher than that from Eq. (6) over the entire range of coverage. At intermediate and high densities, there is a range of θ for which the system is characterized by a LDP. In this range, the coupling between layers is very weak and the 3D configurational entropy per site can be well approximated by that of a 2D system. As it can be observed in the figure, 3D and 2D curves are practically overlapping (within the statistical errors) between $\theta \approx 0.68$ and $\theta = 1$. This result provides a physical interpretation of the IP-LDP transition occurring in the system. At high densities, it is more favorable for the k-mers to occupy spontaneously parallel planes, and the system loses its 3D character and becomes essentially 2D.

The value of the critical density associated to the IP-LDP phase transition, $\theta_{\mathrm{IP-LDP}}$, can be estimated from the minimum value of θ for which occurs the near superposition of the 3D and 2D data. See Fig. 3(b). Here, $\theta_{\mathrm{IP-LDP}}(k = 6) \approx 0.68$, which is consistent with the value reported in Ref. [17]. However, it is important to emphasize that the calculation of the entropy of the LDP from the 2D model is an approximation (especially in the region near the critical densities, where the phase is not completely 2D). A precise determination of $\theta_{\mathrm{IP-LDP}}$ requires an extensive work based on MC simulations and finite-size scaling techniques. This is out of the scope of the present work.

To conclude with the analysis of the case $k = 6$, schematic representations of the different phases that appear on increasing the density are shown in Figs. 4(a) and 4(b): (a) 3D isotropic phase, IP region in Fig. 3(b); and 3(b)

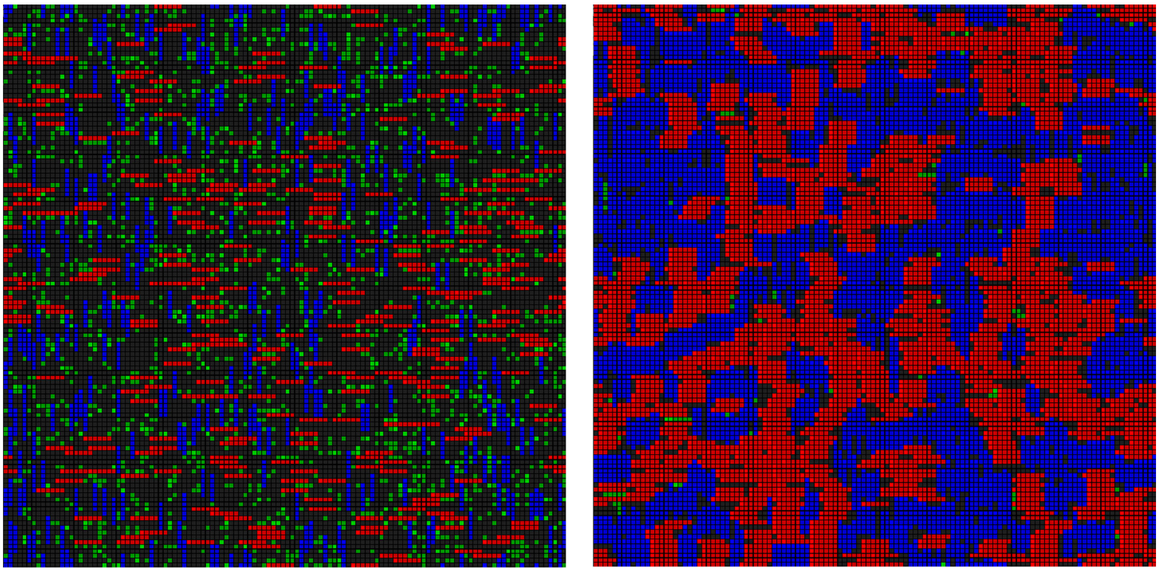
(a) (b)

FIG. 4. (a) Snapshot of a randomly chosen xy plane in the isotropic phase [IP region in Fig. 3(b)]. (b) The same as in part (a), but for an xy plane in the layered-disordered phase [*LDP* region in Fig. 3(b)]. Red and blue squares correspond to units belonging to k-mers lying in the xy plane. Green squares represent units of k-mers lying in a direction perpendicular to the xy plane. Black squares denote empty sites. The configurations shown in parts (a) and (b) have been obtained for lattices with $k = 6$ and $L/k = 20$.

layered-disordered phase, *LDP* region in Fig. 3(b). In spite the fact that the results reported here were obtained for $L/k = 60$, we have chosen $L/k = 20$ (and $k = 6$) for clarity in Figs. 4(a) and 4(b).

We continue studying the case of large k-mers ($k \geqslant 7$). When this condition is satisfied, previous simulation results [17,18] indicate that the system passes through a nematic phase at intermediate concentrations before reaching the high density layered-disordered phase. Thus, the adsorbed layer is in a disordered isotropic phase at low density, shows nematic order at intermediate density, and goes to a layered-disordered phase at high density. As discussed above, the system breaks up into very weakly interacting 2D planes in the LDP. In each plane, the formation of local arrangements (or domains) of parallel k-mers is observed. These domains show mixed orientations, signaling that the long-range orientational order is lost at the high coverage regime. In Ref. [17], the authors also observe the presence of a layered-nematic phase between the nematic and layered-disordered phases. In the layered-nematic phase, the system breaks up into layers, with nematic order in each layer, but very weak correlation between the ordering directions of different layers. Vigneshwar *et al* [17] argued that the layered-nematic phase is a finite-size effect, and in the thermodynamic limit, the nematic phase will have higher entropy per site.

In Fig. 5, the configurational entropy per site has been studied for a system with $k = 7$. The solid line represents analytical results according to expression in Eq. (6) (with $k = 7$). Line and symbols correspond to results produced by MC simulations: 3D simple cubic lattices (line and spheres) and 2D square lattices (line and squares).

For low coverage, the system is isotropic in the sense that the number of k-mers is the same along the d_1, d_2, and d_3 directions, and no orientational order is presented [see Fig. 6(a)]. Then, the 3D entropy is higher than the corresponding ones for 2D square lattices and 1D chains, as it can be seen in Fig. 5(a) (data in the range $0 \leqslant \theta \leqslant 0.4$ are not shown for the sake of clarity).

When the surface coverage is increased, there is a range of densities for which 3D and 1D curves are almost indistinguishable [see Fig. 5(a)]. This is consistent with the presence of nematic order at intermediate values of θ. In this range, the system is characterized by a big domain of parallel k-mers [see Fig. 6(b)] and the configurational entropy per site can be well approximated by Eq. (6). Finally, as the coverage approaches 1, the configurational entropy of the 3D system departs from the corresponding one to the nematic phase, showing the loss of orientational order in the adsorbed phase. In addition, and as was previously observed for $k = 6$, 3D and 2D entropy curves coincide at high density, which suggests the appearance of the LDP in the system [see Fig. 6(c)]. We will return to this point when we discuss the behavior of the configurational entropy per site at full coverage.

The entropy analysis performed in Fig. 5 provides a physical interpretation for the three phases (IP, NP, and LDP) predicted in Refs. [17,18]. This scenery also provides an easy way to estimate the critical densities associated with the IP-NP and NP-LDP phase transitions, $\theta_{\text{IP-NP}}$ and $\theta_{\text{NP-LDP}}$, respectively. As stated in Ref. [15], $\theta_{\text{IP-NP}}$ can be estimated from the minimum value of θ which occurs the near superposition of the 1D and 3D data, while the coverage where 1D and 3D curves separate should be indicative of $\theta_{\text{NP-LDP}}$. In this case, the intersection point between 1D and 3D curves is located around 0.75 [see Fig. 5(a)], and the point where 1D and 3D curves separate is located around 0.92 [see Fig. 5(b)]. These values are not very different from the corresponding values obtained for 2D square lattices: $\theta_{\text{IP-NP}} \approx 0.751$ [10] and $\theta_{\text{NP-LDP}} = 0.917(5)$ [20].

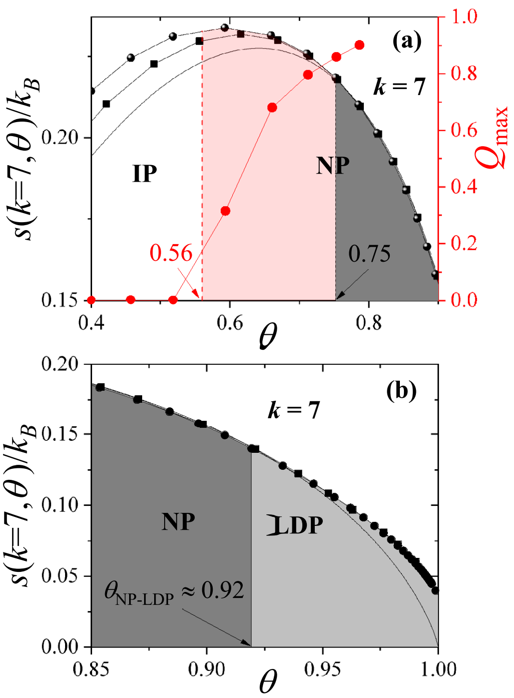

FIG. 5. Configurational entropy per site as function of coverage for straight rigid 7-mers ($k = 7$) adsorbed on three different geometries: 3D simple cubic lattices (line and spheres); 2D square lattices (line and squares) and 1D chains (solid line). Line and symbols correspond to results obtained by MC simulations (complemented by the thermodynamic integration method) and solid line represents analytical results according to expression in Eq. (6) with $k = 7$. The results obtained for low-intermediate density ($0.4 \leqslant \theta \leqslant 0.9$) and high density ($0.85 \leqslant \theta \leqslant 1$) are shown in parts (a) and (b), respectively. In part (a), the nematic order parameter $Q_{\max}$ is plotted as a function of the surface coverage θ (red solid circles, right axis). IP (white), NP (light red and dark gray) and LDP (light gray) regions are shown in the figure.

The value $\theta_{\text{NP-LDP}} \approx 0.92$ agrees also with a previous result in Ref. [17] $\theta_{\text{NP-LDP}} = 0.914(1)$, reinforcing the arguments that the NP-LDP transition is essentially driven by the 2D transition within a layer [17]. The same does not happen with the value estimated from the limit between IP and NP regions $\theta_{\text{IP-NP}} \approx 0.75$, which differs widely from previous reported estimate $\theta_{\text{IP-NP}} \approx 0.556$ [17].

It is important to emphasize that the calculation of the entropy of the nematic phase from the 1D model is an approximation, especially in the region near the IP-NP critical density, where the phase is not completely aligned. This could be the reason of the difference observed in $\theta_{\text{IP-NP}}$. To explore this point, it is helpful to calculate the nematic order parameter Q_i [18]:

$$Q_i = \frac{N_i - \frac{N_j + N_k}{2}}{N} \tag{7}$$

where N_i is the number of rods oriented in the direction d_i ($i \equiv 1, 2, 3$; $N = N_1 + N_2 + N_3$); and (ijk) is a cyclic permutation of (123).

The curve of $Q_{\max} = \max_i(Q_i)$ as a function of the surface coverage θ is shown in Fig. 5(a) (red solid circles, right axis). The data were obtained for $k = 7$, $L/k = 60$, $r_0 = 10^6$ MCs, and $r = 10^6$ MCs. The behavior of $Q_{\max}$ is indicative of the formation of a nematic phase. As found in Ref. [18], $Q_{\max}$ is around 0.2 in the IP-NP critical point. In this case, $Q_{\max} \approx 0.2$ at $\theta \approx 0.56$, which is consistent with previous determinations of $\theta_{\text{IP-NP}}$ [17,18].

The results discussed in the last paragraph allow us to conclude that, in the case of 3D lattices, the alignment at the transition point from the IP phase to the NP phase is low and, consequently, the 1D model does not provide a good approximation to determine $\theta_{\text{IP-NP}}$. On the other hand, $Q_{\max} > 0.9$ in the region where 1D and 3D curves separate, which is consistent with the good prediction of $\theta_{\text{NP-LDP}}$ shown in Fig. 5(b).

Future investigations will be directed to elucidate the structure of the nematic phase at low values of $Q_{\max}$. This task, which is beyond the scope of the present paper, should include more extensive MC calculations and the use of FMT (combined with the nematic order parameter obtained from the simulations).

As mentioned in Sec. I, the relaxation time increases rapidly as the density of the adsorbed k-mers increases and, consequently, MC simulations at high density are very time consuming and may produce artifacts related to inaccurate equilibrium states. The problem is also a much demanding problem from the theoretical point of view: if some sort of correlation exists, like particles that occupy several k contiguous lattice sites, the statistical problem becomes exceedingly difficult. For these reasons, it has been difficult to characterize and study the high-coverage states of adsorbed straight rigid k-mers. In the limit case of $\theta \rightarrow 1$, Dhar and Rajesh [13] showed that the configurational entropy per site of fully packed k-mers on d-dimensional hypercubic lattices follows the law,

$$\frac{s(k, \theta = 1)}{k_B} = k^{-2} \ln k \quad (k \rightarrow \infty). \tag{8}$$

Based on a perturbative series expansion, the authors conjectured that Eq. (8) holds for all $d \geqslant 2$.

Recently, MC simulation [15] and transfer-matrix [16] studies corroborated the validity of Eq. (8) for fully packed rods on 2D square lattices.[1] The same has not happened so far for k-mers in dimensions greater than 2 ($d > 2$). With these ideas in mind, we now propose to get $s(k, \theta \rightarrow 1)/k_B$ for straight rigid $k$mers adsorbed on 3D simple cubic lattices. In the calculations, the curve of $\mu(\theta)$ was integrated following the procedure described in Sec. II. It is important to mention that, because of the weak first-order character of the IP-NP phase transition that occurs for $k \geqslant 7$ [18], a (probably very small) jump is expected in the entropy. However, as will be shown in the following analysis, the thermodynamic integration method provides accurate values of the entropy at full coverage. The results are shown in Fig. 7 for $2 \leqslant k \leqslant 8$.

---

[1] For the case of dimers ($k = 2$), the entropy per site at full coverage has been exactly calculated for the square lattice, $s(k = 2, \theta = 1)/k_B = G/\pi = 0.29156\ldots$ [38]. In addition, a precise estimate $s(k = 3, \theta = 1)/k_B = 0.158520(15)$ has been obtained for trimers on square lattices [39].

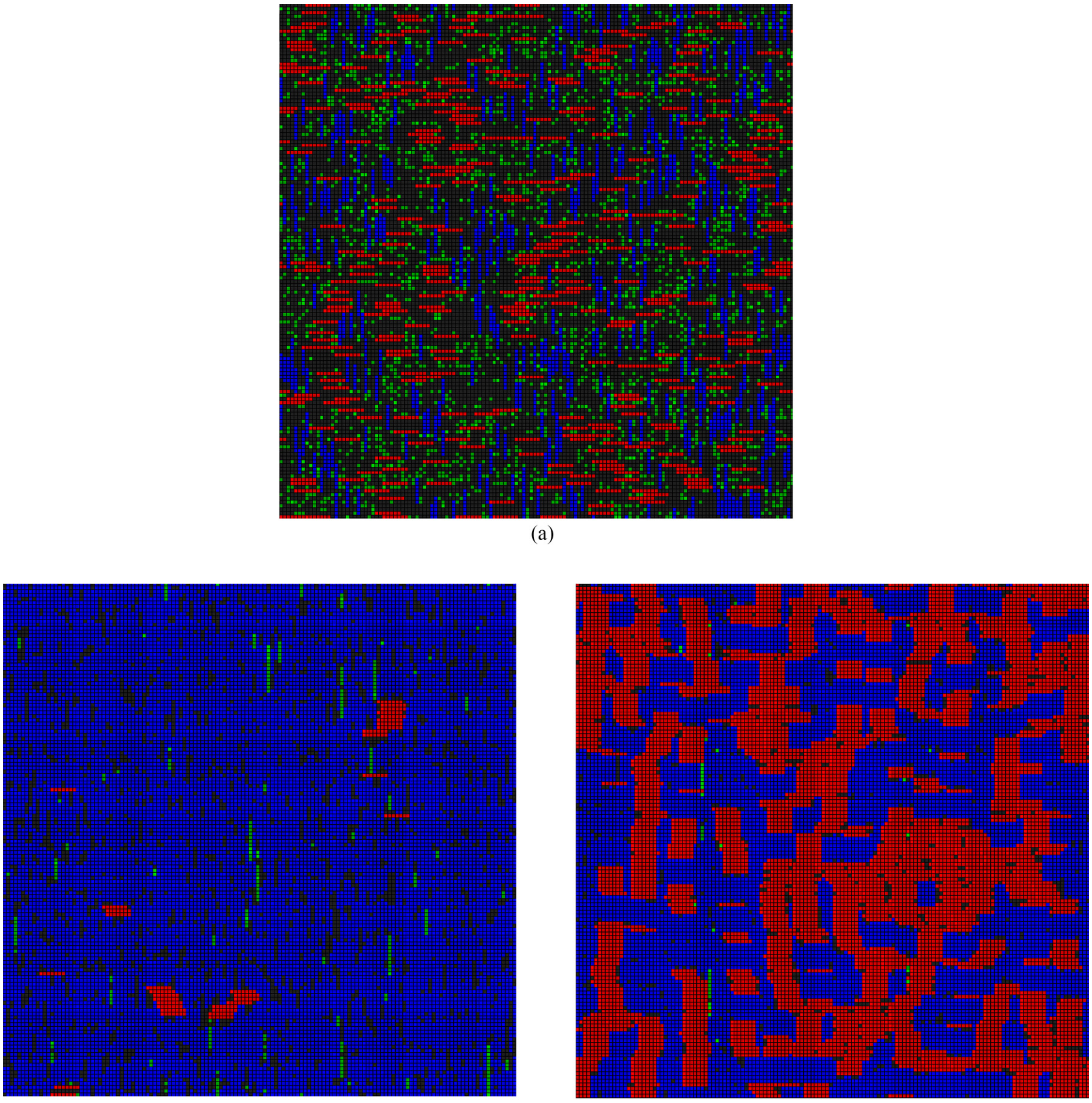

(a)

(b)

(c)

FIG. 6. (a) Snapshot of a randomly chosen xy plane in the isotropic phase [IP region in Fig. 5(a)]. (b) The same as in part (a), but for an xy plane in the nematic phase [NP region in Figs. 3(a) and 3(b)]. (c) The same as in part (a), but for an xy plane in the layered-disordered phase [*LDP* region in Fig. 5(b)]. Red and blue squares correspond to units belonging to k-mers lying in the xy plane. Green squares represent units of k-mers lying in a direction perpendicular to the xy plane. Black squares denote empty sites. The configurations shown in parts (a)–(c) have been obtained for lattices with $k = 7$ and $L/k = 20$.

Spheres represent MC results of this work for 3D simple cubic lattices; open squares correspond to MC data reported in Ref. [15] for 2D square lattices and solid line corresponds to Eq. (8). Numerical and theoretical values are also compiled in Table I.

The data in Fig. 7 show two different regimes. In the range $2 \leqslant k \leqslant 4$, notorious differences are observed between MC data and theoretical results from Eq. (8). As the k-mer size increases, the differences between the MC values and those predicted by Eq. (8) diminish. In the case $k = 5$, the relative difference between MC results and the asymptotic prediction differ less than 9 %. For $k \geqslant 6$, these differences are less than the relative simulation errors. In other words, theoretical and simulation results coincide, within the statistical uncertainty, in the range $k \geqslant 6$. These findings represent the first numerical validation of the expression obtained in Ref. [13] for d-dimensional lattices with $d > 2$.

Another valuable conclusion can be extracted from the data in Fig. 7. For $k \geqslant 5$, 3D MC results are coincident with the results reported in Ref. [15] for 2D square lattices. This finding is consistent with the picture that at high densities and $k \geqslant 5$, the LDP is formed on the lattice. In these conditions, the system will break to two-dimensional layers, with only weak interaction between different layers. As shown in Figs. 3–5, 2D and 3D configurational entropy per site coincide in the high-coverage regime, demonstrating that the 3D problem becomes essentially two-dimensional in the LDP. In this way, the study of configurational entropy developed here physically

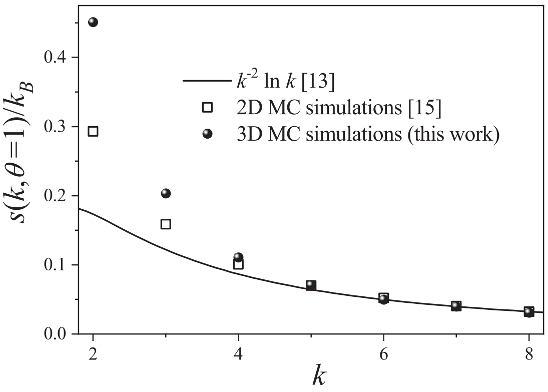

FIG. 7. Configurational entropy per site for straight rigid k-mers at full coverage ($\theta = 1$) as a function of k ($2 \leqslant k \leqslant 8$). Open squares correspond to MC data reported in Ref. [15] for 2D square lattices. Spheres represent MC results obtained in this work for 3D simple cubic lattices. The line indicates theoretical results from Eq. (8) [13].

explains of the apparently surprising fact that the behavior of entropy per site of straight rigid rods at full coverage is superuniversal, and Eq. (8) holds on d-dimensional hypercubic lattices for all $d \geqslant 2$. This is important since the validity of Eq. (8) has been conjectured and has not yet been rigorously proved [13].

IV. CONCLUSIONS

In the present work, we have addressed the critical properties of straight rigid k-mers deposited on a simple cubic lattice. The adsorption process was analyzed in terms of the configurational entropy of the adsorbed phase. The results were obtained by combining Monte Carlo simulations in the grand canonical ensemble and thermodynamic integration method.

Special attention was devoted to the study of the configurational entropy per site at full coverage $s(k, \theta = 1)/k_B$. Using MC simulations and thermodynamic integration method, the dependence of $s(k, \theta = 1)/k_B$ on k-mer size was got (in the range $2 \leqslant k \leqslant 8$) and compared with the recently reported expression: $s(k, \theta = 1)/k_B = k^{-2} \ln k \quad (k \to \infty)$ [13]. The comparison analysis revealed that, for $k \geqslant 6$, simulation and theoretical results coincide within the statistical uncertainty. The MC study presented here represents the first numerical validation of the theoretical prediction of Rajesh and Dhar [13] for d-dimensional lattices with $d > 2$ and allows for an accurate determination of its validity range.

The configurational entropy per site of the adsorbed phase was also calculated over the entire coverage range ($0 \leqslant \theta \leqslant 1$). For each value of k ($2 \leqslant k \leqslant 8$), the results obtained for 3D simple cubic lattices were compared with those corresponding to 1D lattices and 2D square lattices with two allowed orientations. The comparison between 1D, 2D and 3D entropy curves allowed us to explore the different phases (and orientational transitions) that appear on the surface with increasing the density of adsorbed k-mers. Based on this study (and previous research), the following conclusions can be drawn.

In the range $2 \leqslant k \leqslant 4$, the 3D entropy is greater than those of 2D and 1D systems over the entire range of coverage. This means that, according to the maximum entropy principle, the adsorbed layer is characterized by an isotropic phase (where the k-mers are equally distributed in the three directions of space) and reaches neither nematic nor layered order at any point when the density varies between 0 and 1. MC data were also compared with FMT, which in this case is equivalent to the DiMarzio's theory for an isotropic distribution of rods [31]. The excellent agreement between simulation and theoretical results indicates that FMT is a good approximation for a state with zero nematic order.

For $k \geqslant 5$, the adsorbed layer goes to a LDP at high densities. In this regime, 3D and 2D entropy curves are practically overlapping, indicating that the coupling between layers is very weak and the 3D configurational entropy per site can be well approximated by that of a 2D system. Clearly, it is more favorable for the k-mers (with $k \geqslant 5$) to occupy spontaneously parallel planes, and the system loses its 3D character and becomes essentially 2D. In other words, our results demonstrate that the layered-disordered phase is essentially a 2D phase. This finding is the key to understanding the main characteristics of the system at full coverage and allows us to obtain a physical interpretation of the superuniversal behavior of the configurational entropy per site of fully packed large rods on d-dimensional hypercubical lattices.

With $k = 5$ and $k = 6$, the LDP is preceded by an isotropic phase with similar characteristics to that observed for $k \leqslant 4$, and occurring at low and intermediate densities. For higher values of k ($k \geqslant 7$), a nematic phase appears between the low-coverage IP and the high-coverage LDP.

Finally, the critical densities separating the different adsorbed phases were estimated from the entropy analysis. The values obtained for the critical points associated to the IP-LDP transition ($k = 5, 6$) and to the NP-LDP transition ($k \geqslant 7$) are consistent with previous determinations in the literature [17]. For the IP-NP transition ($k \geqslant 7$), the value of the critical density estimated from the intersection point between 1D and 3D entropy curves is higher than the calculated one in Ref. [17]. The study of the nematic order parameter Q [18] revealed that the alignment at the transition point from the IP phase to the NP phase is low and, consequently, the 1D model of the nematic phase does not provide a good approximation to determine $\theta_{\text{IP-NP}}$.

Future efforts will be done following two directions: (1) using information theory [10,11] and finite size scaling analysis, to develop a complete study of the phase transitions occurring in the adsorbed layer with increasing density; and (2) to extend the present analysis to the problem of cuboids on d-dimensional hypercubical lattices, where a much richer phase diagram is expected.

ACKNOWLEDGMENTS

This work was supported in part by CONICET (Argentina) under project number PIP 112-201101-00615; Universidad Nacional de San Luis (Argentina) under Project No. 03-1920; CEDENNA (Chile) under contract ANID AFB220001 and Fondecyt (Chile) under contract 1230055. The numerical work were done using the BACO parallel cluster [40] located at Instituto de Física Aplicada, Universidad Nacional de San Luis-CONICET, San Luis, Argentina.

[1] L. Onsager, The effects of shape on the interaction of colloidal particles, Ann. N.Y. Acad. Sci. **51**, 627 (1949).

[2] P. J. Flory, Statistical thermodynamics of semi-flexible chain molecules, Proc. R. Soc. A **234**, 60 (1956).

[3] R. Zwanzig, First-order phase transition in a gas of long thin rods, J. Chem. Phys. **39**, 1714 (1963).

[4] A. Ghosh and D. Dhar, On the orientational ordering of long rods on a lattice, Europhys. Lett. **78**, 20003 (2007).

[5] D. A. Matoz-Fernandez, D. H. Linares, and A. J. Ramirez-Pastor, Determination of the critical exponents for the isotropic-nematic phase transition in a system of long rods on two-dimensional lattices: Universality of the transition, Europhys. Lett. **82**, 50007 (2008).

[6] D. A. Matoz-Fernandez, D. H. Linares, and A. J. Ramirez-Pastor, Critical behavior of long linear k-mers on honeycomb lattices, Physica A **387**, 6513 (2008).

[7] M. Disertori and A. Giuliani, The nematic phase of a system of long hard rods, Commun. Math. Phys. **323**, 143 (2013).

[8] D. Dhar, R. Rajesh, and J. F. Stilck, Hard rigid rods on a bethe-like lattice, Phys. Rev. E **84**, 011140 (2011).

[9] K. Padavala, A. Singh, and J. Kundu, Machine learned phase transitions in a system of anisotropic particles on a square lattice, arXiv:2102.03006.

[10] E. E. Vogel, G. Saravia, and A. J. Ramirez-Pastor, Phase transitions in a system of long rods on two-dimensional lattices by means of information theory, Phys. Rev. E **96**, 062133 (2017).

[11] E. E. Vogel, G. Saravia, A. J. Ramirez-Pastor, and P. M. Pasinetti, Alternative characterization of the nematic transition in deposition of rods on two-dimensional lattices, Phys. Rev. E **101**, 022104 (2020).

[12] A. Shah, D. Dhar, and R. Rajesh, Phase transition from nematic to high-density disordered phase in a system of hard rods on a lattice, Phys. Rev. E **105**, 034103 (2022).

[13] D. Dhar and R. Rajesh, Entropy of fully packed hard rigid rods on d-dimensional hypercubic lattices, Phys. Rev. E **103**, 042130 (2021).

[14] N. D. Gagunashvili and V. B. Priezzhev, Close packing of rectilinear polymers on a square lattice, Theor. Math. Phys. **39**, 507 (1979).

[15] P. M. Pasinetti, A. J. Ramirez-Pastor, E. E. Vogel, and G. Saravia, Entropy-driven phases at high coverage adsorption of straight rigid rods on two-dimensional square lattices, Phys. Rev. E **104**, 054136 (2021).

[16] L. R. Rodrigues, J. F. Stilck, and W. G. Dantas, Entropy of rigid k-mers on a square lattice, Phys. Rev. E **107**, 014115 (2023).

[17] N. Vigneshwar, D. Dhar, and R. Rajesh, Different phases of a system of hard rods on three dimensional cubic lattice, J. Stat. Mech. (2017) 113304.

[18] A. Gschwind, M. Klopotek, Y. Ai, and M. Oettel, Isotropic-nematic transition for hard rods on a three-dimensional cubic lattice, Phys. Rev. E **96**, 012104 (2017).

[19] J. Kundu, R. Rajesh, D. Dhar, and J. F. Stilck, A Monte Carlo algorithm for studying phase transition in systems of hard rigid rods, AIP Conf. Proc. **1447**, 113 (2012).

[20] J. Kundu, R. Rajesh, D. Dhar, and J. F. Stilck, Nematic-disordered phase transition in systems of long rigid rods on two-dimensional lattices, Phys. Rev. E **87**, 032103 (2013).

[21] A. J. Ramirez-Pastor, T. P. Eggarter, V. D. Pereyra, and J. L. Riccardo, Statistical thermodynamics and transport of linear adsorbates, Phys. Rev. B **59**, 11027 (1999).

[22] D. Nicholson and N. D. Parsonage, *Computer Simulation and the Statistical Mechanics of Adsorption* (Academic Press, London, 1982).

[23] K. Binder, *Applications of the Monte Carlo Method in Statistical Physics*, Topics in Current Physics Vol. 36 (Springer, Berlin, 1984).

[24] K. Binder, Static and dynamic critical phenomena of the two-dimensional q-state Potts model, J. Stat. Phys. **24**, 69 (1981).

[25] T. L. Polgreen, Monte Carlo simulation of the fcc antiferromagnetic Ising model, Phys. Rev. B **29**, 1468 (1984).

[26] J. P. Hansen and L. Verlet, Phase transitions of the lennard-jones system, Phys. Rev. **184**, 151 (1969).

[27] F. Romá, A. J. Ramirez-Pastor, and J. L. Riccardo, Configurational entropy for adsorbed linear species (k-mers), J. Chem. Phys. **114**, 10932 (2001).

[28] F. Romá, A. J. Ramirez-Pastor, and J. L. Riccardo, Configurational entropy in k-mer adsorption, Langmuir **16**, 9406 (2000).

[29] W. H. Press, B. P. Flannery, S. A. Teukolsky, and W. T. Vetterling, *Numerical Recipes in C: The Art of Scientific Computing* (Cambridge University Press, Cambridge, 1992).

[30] E. A. Guggenheim, Statistical thermodynamics of mixtures with zero energies of mixing, Proc. R. Soc. London A **183**, 203 (1944).

[31] E. A. DiMarzio, Statistics of orientation effects in linear polymer molecules, J. Chem. Phys. **35**, 658 (1961).

[32] M. A. Cotter and D. E. Martire, A quasi-chemical lattice treatment of rod-like molecules. application to the nematic-Isotropic transition, Mol. Cryst. Liq. Cryst. **7**, 295 (1969).

[33] L. Lafuente and J. A. Cuesta, Fundamental measure theory for lattice fluids with hard-core interactions, J. Phys.: Condens. Matter **14**, 12079 (2002).

[34] L. Lafuente and J. A. Cuesta, Density Functional Theory for General Hard-Core Lattice Gases, Phys. Rev. Lett. **93**, 130603 (2004).

[35] Y. Rosenfeld, Free-Energy Model for the Inhomogeneous Hard-Sphere Fluid Mixture and Density-Functional Theory of Freezing, Phys. Rev. Lett. **63**, 980 (1989).

[36] Y. Rosenfeld, Density functional theory of molecular fluids: Free-energy model for the inhomogeneous hard-body fluid, Phys. Rev. E **50**, R3318(R) (1994).

[37] M. Oettel, M. Klopotek, M. Dixit, E. Empting, T. Schilling, and H. HansenGoos, Monolayers of hard rods on planar substrates. I. Equilibrium, J. Chem. Phys. **145**, 074902 (2016).

[38] M. E. Fisher, Statistical mechanics of dimers on a plane lattice, Phys. Rev. **124**, 1664 (1961).

[39] A. Ghosh, D. Dhar, and J. L. Jacobsen, Random trimer tilings, Phys. Rev. E **75**, 011115 (2007).

[40] Available at http://cluster_infap.unsl.edu.ar/wordpress.